IDENTIFICATION OF GROUNDWATER BASIN SHAPE AND BOUNDARY USING HYDRAULIC TOMOGRAPHY

Kwankwai Daranond[1*]; Tian-Chyi Jim Yeh[1]

[1]University of Arizona, Department Hydrology and Atmospheric Sciences. 1133 E. James E. Rogers Way JW Harshbarger Building, Tucson, AZ, USA 85721.

E-mail: daranondk@email.arizona.edu - Tel: + 1 (520) 270-0921 (*Corresponding author)

Abstract

Shapes and boundary types of a groundwater basin play important roles in groundwater management and contaminant migration issues. Hydraulic tomography (HT) is a recently developed new approach for high-resolution characterization of aquifers. HT is not only an inverse methodology but also a logic data collection approach to integrating non-fully redundant hydraulic information to provide high-resolution characterizations of aquifers. In this study, HT was applied to synthetic 2-D aquifers to investigate its feasibility to map the irregular shapes and types of the aquifer boundaries. We first used the forward model of VSAFT2 to simulate hydraulic responses of aquifers due to pumping tests under combinations of irregular shaped boundary conditions, e.g., constant head, flux, and no-flow boundaries. Then, we used SimSLE (Simultaneous Successive Linear Estimator) inverse model in VSAFT2 to estimate the spatial distribution of hydraulic properties within rectangular shaped domains with constant head boundaries. The simulations were conducted in both steady and transient state using different monitoring network to assess the ability of HT with the different network for detecting types and shapes of the boundary. Furthermore, the improvement of the estimation with prior information of T was also investigated. These cases were investigated using Monte Carlo simulations to ensure statistical meaningful conclusions.

Keyword: groundwater basin, hydraulic tomography, 2-D model, boundary.

Introduction

The spatial distribution of hydraulic properties is significant for issues of groundwater management and contaminant transport. Many analytical solutions were created to estimate hydraulic parameters, for instance, the Theis solution (Theis, 1935) and Cooper-Jacob solution (Cooper and Jacob, 1946). However, some assumptions of these analytical solutions might not be found in the real world, especially the assumption of homogeneity and the infinite extent of the aquifer. In a couple of decades, numerical solutions have been developed to deal with more complicated calculation and more detailed of the spatial distribution of hydraulic properties. In this study, the method of Hydraulic Tomography (HT) (Yeh and Liu, 2000) in two-dimension is employed to investigate the aquifer heterogeneity. HT is considered to be a cost-effective method (Ni et al., 2009) due to the series of pumping test that allowing us to obtain more head data from the limited number of installed wells. Many experiments of HT were taken both in a laboratory sandbox (e.g., Liu et al., 2002; Liu et al., 2007; Yin and Illman, 2009) and field study (e.g., Straface et al., 2007; Wen et al., 2010; Berg and Illman, 2012; Zha et al., 2016). Their studies indicate that HT can characterize the detailed aquifer heterogeneity including geological structure such as fault and fracture.

The boundary condition is essential to determine the uniqueness of a solution of the governing equation of groundwater flow, which is a second-order partial differential equation (Reilly, 2001). In this study, we investigate the effect of using an incorrect boundary condition. The conceptual model of buried valley aquifer is applied to our simulation. This type of aquifer is generally located in North America and Europe where were glaciated in the past (Cummings et al., 2012; Kehew et al., 2012; Baechler, 2017). Subglacial meltwater eroded rock or sediment surface beneath the ice sheet and carved the host rock into the tunnel shape. The tunnel of impermeable substratum was filled with sequences of coarse- and fine-grained sediment (Høyer er al., 2015). We synthesize the 2-D buried valley model by substitution the impermeable area with no-flow boundary and channel area with constant head boundary. The material inside the domain is heterogeneous. Wells are installed and a series of pumping tests are conducted to obtain the observation data of drawdown in the domain. Then, we create the scenarios that might possibly occur in a field study which are the impermeable parts are buried beneath the surface and they cannot be visually detected on the surface. This leads to the question for an inverse model that: can we assign constant head boundaries to the invisible impermeable material? How well can we estimate the material inside the domain when using incorrect boundary? And whether HT can detect the impermeable part?

To improve the estimation of hydraulic properties, prior knowledge of the aquifer, such as transmissivity (T), flux (q), correlation length (λ), or geological structure is needed (Tso et al., 2016; Zha et al., 2017). In this experiment, the prior information of the transmissivity is applied to the inverse model. We compare between using uniform T initial guess, which

is the value of mean T, and non-uniform T, which is obtained from the estimation in steady state. We also examine the roles of geologic information: 1) The geologic information in the study area is not considered. The prior knowledge of T does not present any zone of low permeability. 2) The information of geology of the buried valley area are known; the rock formations are approximately described as low transmissivity zones.

Materials and Methods

Model Setup

A 2-dimension horizontal forward model is synthesized with an irregular domain (Fig. 1a) by using a graphic user interface of VSAFT2 (Variably Saturated Flow and Transport utilizing the Modified Method of Characteristics, in 2-D) (Yeh et al., 1993). Left- and right-boundary are designed as no-flow boundaries representing zones of the impermeable formation. Top- and bottom-boundary are assigned as constant head boundaries portraying the channel between the buried valley. Nine monitoring wells are penetrated into the channel region. Red and black circles indicate the location of the pumping-monitoring wells and monitoring wells, respectively. Five individual pumping tests are conducted sequentially; the observation data are collected from eight observation wells in each stress. Fig. 1b and 1c are the 50x50 grid cell size with 4m spacing domains designed for the inverse model. The boundaries of the domain are incorrectly specified as constant head boundaries following the scenario that the impermeable substratum cannot be seen from the surface. Fig. 1b represents the situation when the geology information is not considered. On the other hand, Fig. 1c displays the black zones, which were approximately delineated describing the impermeable zones with low transmissive material.
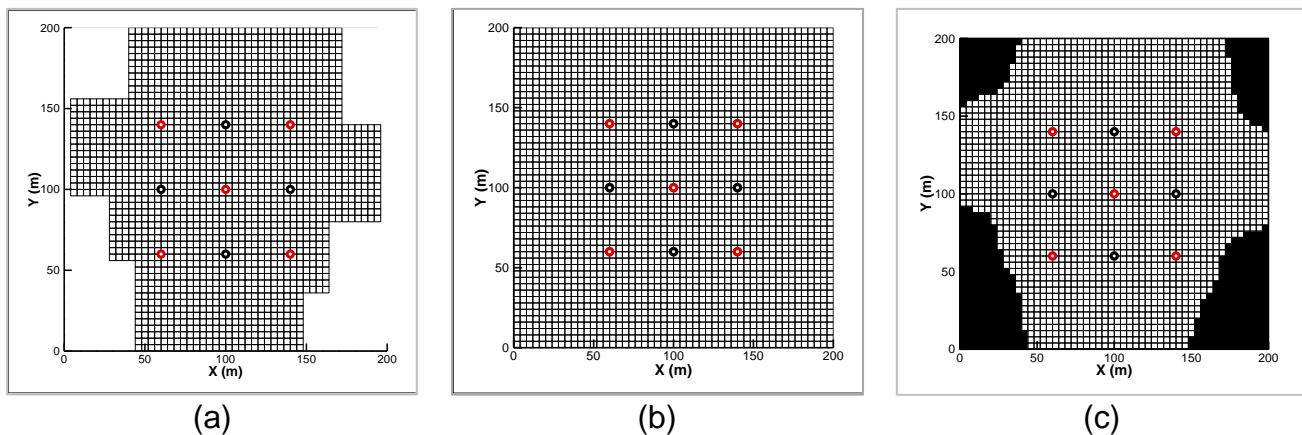

(a)   (b)   (c)

Figure 1. Model domain for the simulation of (a) forward model and (b), (c) inverse model

The random field of transmissivity (T) and storage coefficient (S) is generated by using the stochastic concept (Yeh, 1992, Yeh et al., 2015). The spatial distribution is described by mean lnT, variance lnT, and correlation length. The isotropic material (Fig. 2a and 2b) is synthesized with mean lnT and mean lnS, -1.498 m^2/d and -7.457 [-], respectively. Variances of lnT and lnS are 1.61 and 1.10; they describe the variation of T and S from

the mean value. The correlation length in X and Y axes are 50 m indicating the geometry of aquifer in X and Y direction. Pumping wells and monitoring wells are fully penetrated into the synthetic aquifer.

The characteristics of groundwater flow in a two-dimensional, depth-averaged, saturated medium can be described as a governing partial differential equation:

$$\nabla \cdot [T(\boldsymbol{x})\nabla H] + Q(\boldsymbol{x}_p) = S(\boldsymbol{x})\frac{\partial H}{\partial t} \tag{1}$$

base on the boundary and initial conditions:

$$H|_{\Gamma 1} = H_1, \ [\,T(\boldsymbol{x})\nabla H\,] \cdot \boldsymbol{n}|_{\Gamma 2} = q \quad \text{and} \quad H|_{t=0} = H_0 \tag{2}$$

where $T(\mathbf{x})$ is the transmissivity [L^2/T], $\overline{H}$ is the total head [L], $Q(\mathbf{x}_p)$ is the pumping rate [L^3/T] at location $\mathbf{x}_p$, $S(\mathbf{x})$ is the storage coefficient [-], H_1 is the prescribed total head at Dirichlet boundary Γ_1, q is the prescribed flux at the Neumann boundary Γ_2, $\boldsymbol{n}$ is a unit vector normal to the boundary, and H_0 is the total head before applying any stress to the aquifer.
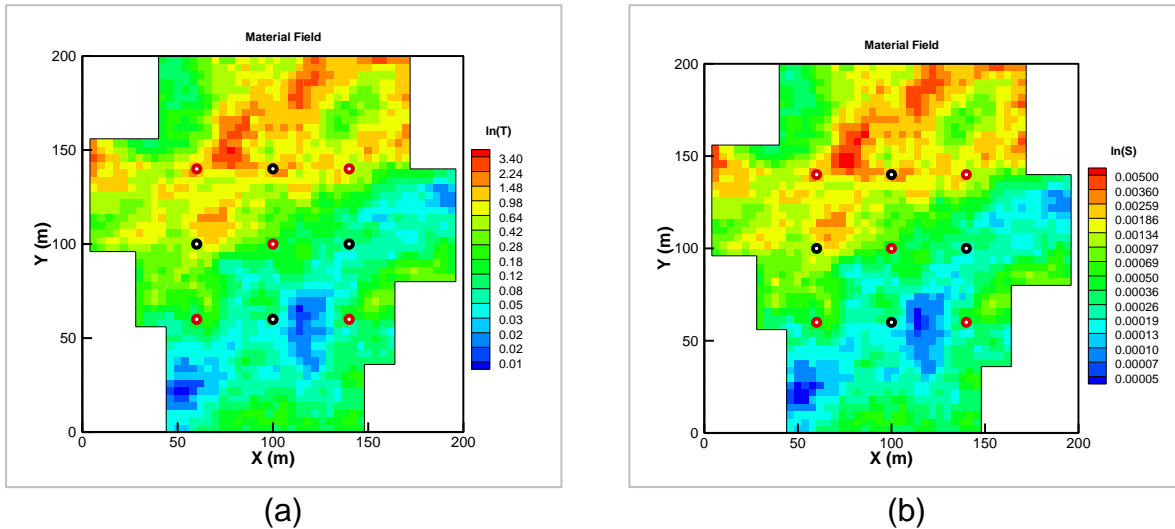

Figure 2. The same realization of (a) transmissivity and (b) storage coefficient.

Hydraulic Tomography Analysis

The collected simulated head data form multiple pumping tests are considered at once in order to estimate T and S with Simultaneous Successive Linear Estimator (SimSLE) (Xiang et al., 2009) inverse model in VSAFT2. As SimSLE requires the prior information of mean, variance, and correlation length of material properties, we focus on different data of prior T and S to evaluate the estimates in the channel part of the buried valley. We study two major approaches: for Case A, we use the square domain with one T distribution zone (Fig. 1b); and for case B, we use the square domain with two T distribution zones (Fig. 1c). Inverse models are performed in both steady and transient

4

state. The estimation of T from the steady state will be applied as the non-uniform prior information or initial guess for the transient state inverse model.

Case 1 Uniform Initial Guess of T and True S (1A, 1B): The true distribution of S is used as prior information; we only estimate T to reduce the number of parameters in the estimation. The prior information of T is the uniform distribution. The identical value of average T of true material over the domain is assigned.

Case 2 Non-uniform Initial guess of T and True S (2A, 2B): This case also applies the distribution of true S to the inverse model. The initial guess of T, in this case, is non-uniform; the T distribution obtained from the estimation in steady state.

Case 3 Uniform Initial Guess of T and S (3A, 3B): The uniform distribution of prior information is defined by average values of T and S of the true material.

Case 4 Non-uniform Initial Guess of T and Uniform Initial Guess of S (4A, 4B): The estimated T from the steady state is further applied to this case with the uniform distribution of the average value of true S.

Performance Metrics

To evaluate the HT inverse model, the true values of T are plotted against the estimate; the regression model is applied. The criteria of the coefficient of determination (R^2), the mean absolute error (L_1), the mean square error (L_2), the slope, and intercept, which produce the best linear fit, are taken into account. L_1 and L_2 can be described as the following equations:

$$L_1 = \frac{1}{N}\sum_{i=1}^{N}|x_i - \hat{x}_i| \tag{3}$$

$$L_2 = \frac{1}{N}\sum_{i=1}^{N}(x_i - \hat{x}_i)^2 \tag{4}$$

where N is the total number of elements, *i* is the element number, x_i is the true T value at the element *i* th, and $\hat{x}_i$ is the estimated T value at the element *i* th.

In general, the higher R^2 indicates a better result; the lower L_1, L_2, the better of the estimates. The slope that closes to 1 is likely to parallel to the true distribution; the approaching to zero intercepts are the better.

Results and Discussion

The statistics data for each case are summarized in Table 1. These numbers are based on the calculation from a single realization or one possibility of the heterogeneity of the assigned mean, variance, and correlation length. Only the data point inside the irregular boundary is used in the calculation.

5

With one realization, we cannot make a conclusion that which model is better than another. Only 3 of 5 cases in two-zone materials have higher R^2 and lower L_1 and L_2 than one-zone material. The non-uniform initial guess obtained from the steady state cannot clearly indicate that it helps the inverse model to improve the estimation in this realization. However, despite the incorrect boundary that we assigned to the inverse model, HT estimation can capture the general trends of low T and high T material inside the irregular domain. Moreover, it can capture the no-flow boundary. Although the results of the estimation cannot delineate the exact region of the impermeable boundaries, the model represents the area along the no-flow boundaries with low T zones (blue areas close to the left- and right-boundary in Fig. 3 and Fig. 4).

Table 1. Statistics of one realization of a heterogeneous aquifer.

Performance metrics	R^2	L_1	L_2	Slope	Intercept
1 Zone					
Steady state (Uniform T)	0.60421	0.77713	1.1327	0.92387	-0.587308
1A (Uniform T, True S)	0.54351	0.68621	1.2064	0.87916	-0.553439
2A (Non-uniform T, True S)	0.6413	0.63442	0.8673	0.90559	-0.480715
3A (Uniform T and S)	0.60327	0.68261	0.98389	0.90007	-0.482603
4A (Non-uniform T, Uniform S)	0.58929	0.78298	1.1688	0.91392	-0.59845
2 Zones					
Steady state (Uniform T)	0.56457	0.66892	0.83307	0.68725	-0.768085
1B (Uniform T, True S)	0.63523	0.57958	0.80137	0.8745	-0.451869
2B (Non-uniform T, True S)	0.62672	0.56983	0.84331	0.87976	-0.460314
3B (Uniform T and S)	0.67481	0.56678	0.65214	0.84551	-0.475503
4B (Non-uniform T, Uniform S)	0.6439	0.66283	1.0014	0.9633	-0.471829

As we cannot make a conclusion from a single realization, initially, we simulate other nine realizations to investigate the general picture of this experiment. Fig. 5 shows that simulations of two-zone materials have better statistics: higher R^2, lower L_1, L_2, and intercept values. The case that has the best statistics values based on these ten realizations is case 3, uniform T and S. This indicates that the prior information from the steady state estimation and the role of true S as the initial guess are not significant to perform an inverse model. However, all of the results are dependent only on ten scenarios of heterogeneity distribution.
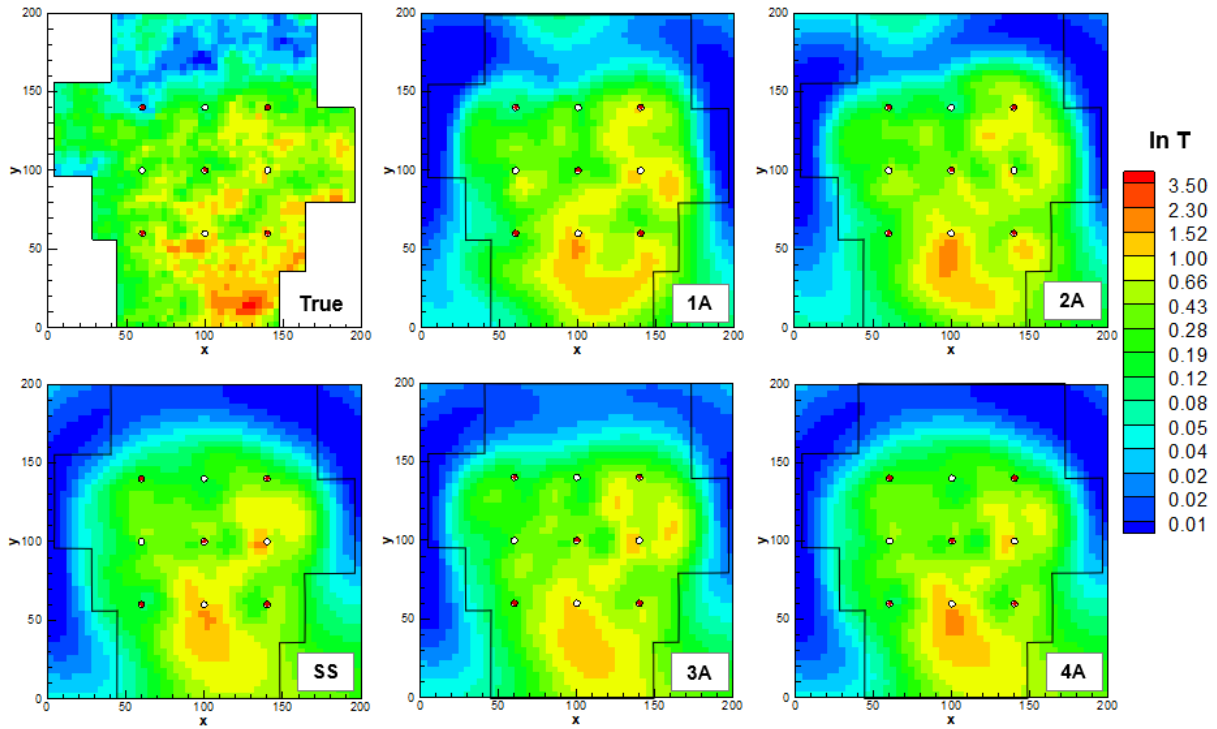
Figure 3. True T field comparing with one-zone case estimated T fields in logarithmic scale.
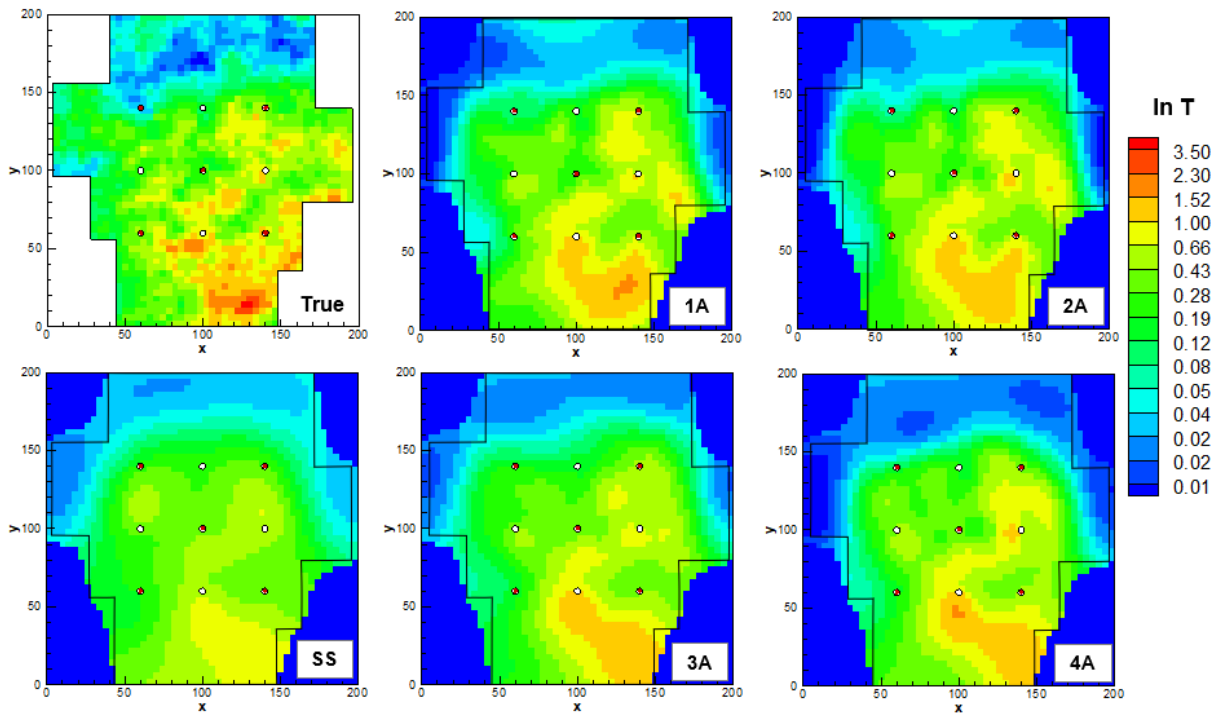(SS is steady state)

Figure 4. True T field comparing with two-zone case estimated T fields in logarithmic scale.
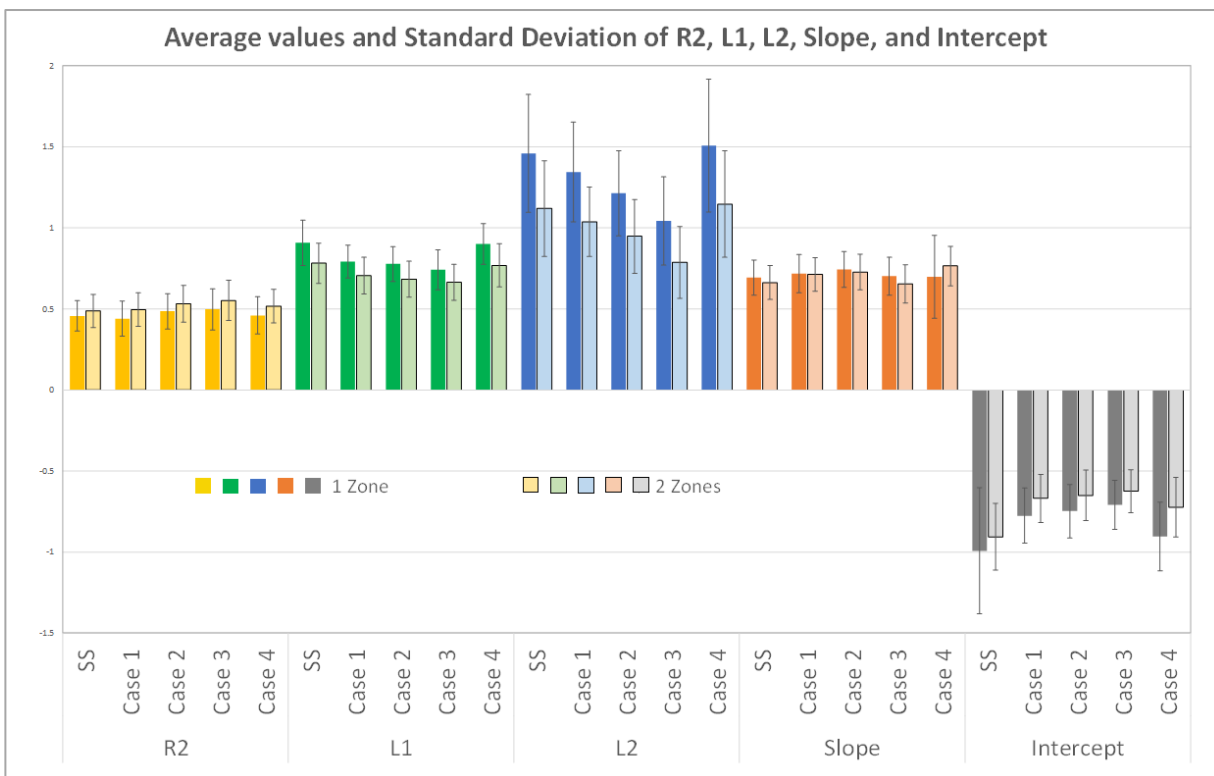(SS is steady state)

7

Figure 5. Average and standard deviation of performance metrics of ten realizations comparing between one-zone and two-zone cases.

Conclusion

We can obtain more head data from the limited number of groundwater well by using HT method. The collected observed head data at different location contain the information of the heterogeneity of the aquifer as well as the boundary. The no-flow boundary or the impermeable formation of rock will be represented as low transmissive area. The knowledge of geology and structure in the study area can help to improve the estimation. However, more realizations have to be considered to make a more robust conclusion about the role of the prior information.

References

Baechler, F. (2017). The geology and hydrogeology of buried bedrock valley aquifers on Cape Breton Island, Nova Scotia: an overview. *Atlantic Geology*, 53, pp.301-324.

Berg, S. and Illman, W. (2012). Field Study of Subsurface Heterogeneity with Steady-State Hydraulic Tomography. *Ground Water*, 51(1), pp.29-40.

Cooper, H. and Jacob, C. (1946). A generalized graphical method for evaluating formation constants and summarizing well-field history. *Transactions, American Geophysical Union*, 27(4), p.526.

8

Cummings, D., Russell, H. and Sharpe, D. (2012). Buried-valley aquifers in the Canadian Prairies: geology, hydrogeology, and origin1Earth Science Sector (ESS) Contribution 20120131. *Canadian Journal of Earth Sciences*, 49(9), pp.987-1004.

Høyer, A., Jørgensen, F., Sandersen, P., Viezzoli, A. and Møller, I. (2015). 3D geological modelling of a complex buried-valley network delineated from borehole and AEM data. *Journal of Applied Geophysics*, 122, pp.94-102.

Kehew, A., Piotrowski, J. and Jørgensen, F. (2012). Tunnel valleys: Concepts and controversies — A review. *Earth-Science Reviews*, 113(1-2), pp.33-58.

Liu, S., Yeh, T. and Gardiner, R. (2002). Effectiveness of hydraulic tomography: Sandbox experiments. *Water Resources Research*, 38(4), pp.5-1-5-9.

Liu, X., Illman, W., Craig, A., Zhu, J. and Yeh, T. (2007). Laboratory sandbox validation of transient hydraulic tomography. *Water Resources Research*, 43(5).

Ni, C., Yeh, T. and Chen, J. (2009). Cost-Effective Hydraulic Tomography Surveys for Predicting Flow and Transport in Heterogeneous Aquifers. *Environmental Science & Technology*, 43(10), pp.3720-3727.

Reilly, T.E. (2001). System and boundary conceptualization in ground-water flow simulation: *U.S. Geological Survey Techniques of Water-Resources Investigations*, Book 3, Chapter B8, 26 p

Straface, S., Yeh, T., Zhu, J., Troisi, S. and Lee, C. (2007). Sequential aquifer tests at a well field, Montalto Uffugo Scalo, Italy. *Water Resources Research*, 43(7).

Theis, C. (1935). The relation between the lowering of the Piezometric surface and the rate and duration of discharge of a well using ground-water storage. *Transactions, American Geophysical Union*, 16(2), p.519.

Tso, M. C., Zha, Y., Yeh, T. and Wen, J. (2016). The relative importance of head, flux, and prior information in hydraulic tomography analysis. *Water Resources Research*, 52(1), pp.3-20.

Wen, J., Wu, C., Yeh, T. and Tseng, C. (2010). Estimation of effective aquifer hydraulic properties from an aquifer test with multi-well observations (Taiwan). *Hydrogeology Journal*, 18(5), pp.1143-1155.

Xiang, J., Yeh, T. J., Lee, C., Hsu, K., & Wen, J. (2009). A simultaneous successive linear estimator and a guide for hydraulic tomography analysis. *Water Resources Research,45*(2). doi:10.1029/2008wr007180

Yeh, T., Khaleel, R., Carroll, K.C.. (2015). Flow Through Heterogeneous Geological Media, *Cambridge University Press*, Cambridge

Yeh, T. and Liu, S. (2000). Hydraulic tomography: Development of a new aquifer test method. *Water Resources Research*, 36(8), pp.2095-2105.

Yeh, T., Srivastava, R., Guzman, A., Harter, T. (1993). A Numerical Model for Water Flow and Chemical Transport in Variably Saturated Porous Media. *Ground Water*, 31(4), pp.634-644.

Yeh, T. (1992). Stochastic modeling of groundwater flow and solute transport in aquifers. *Hydrological Processes*, 6(4), pp.369-395.

Yin, D. and Illman, W. (2009). Hydraulic tomography using temporal moments of drawdown recovery data: A laboratory sandbox study. *Water Resources Research*, 45(1).

Zha, Y., Yeh, T., Illman, W., Onoe, H., Mok, C., Wen, J., Huang, S. and Wang, W. (2017). Incorporating geologic information into hydraulic tomography: A general framework based on geostatistical approach. *Water Resources Research*, 53(4), pp.2850-2876.

Zha, Y., Yeh, T., Illman, W., Tanaka, T., Bruines, P., Onoe, H., Saegusa, H., Mao, D., Takeuchi, S. and Wen, J. (2016). An Application of Hydraulic Tomography to a Large-Scale Fractured Granite Site, Mizunami, Japan. *Groundwater*, 54(6), pp.793-804.